Journal of Membrane Science, 64 (1991) 1-11
Elsevier Science Publishers B.V., Amsterdam

Microporous membrane formation via thermally-induced phase separation. II. Liquid–liquid phase separation

Douglas R. Lloyd[a], Sung Soo Kim[a] and Kevin E. Kinzer[b]
[a]*Department of Chemical Engineering, Separations Research Program, Center for Polymer Research, The University of Texas at Austin, Austin, TX 78712 (USA)*
[b]*3M Corporate Research, 219-1-01 3M Center, St. Paul, MN 55144 (USA)*

(Received December 11, 1990; accepted in revised form May 8, 1991)

Abstract

Microporous membranes have been prepared via thermally-induced liquid-liquid phase separation of isotactic polypropylene-n,n-bis (2-hydroxyethyl) tallowamine mixtures. The thermally-induced phase separation process is discussed in terms of the thermodynamics of the binary mixture and possible phase separation mechanisms. It is demonstrated that membranes can be produced by liquid-liquid phase separation followed by solidification of the polymer or by solid-liquid phase separation.

Keywords: membrane preparation and structure; microporous membranes; phase separation, thermally induced; phase separation, liquid-liquid

Introduction

In the previous paper in this series [1], the process for microporous membrane preparation via thermally-induced phase separation, TIPS, was described with particular attention given to solid–liquid phase separation. Briefly, the TIPS process consists of the following steps:
1. A homogeneous solution is formed at an elevated temperature by blending the polymer with a high-boiling, low molecular weight liquid or solid diluent. The initial temperature (T_i) must be less than the boiling point of the diluent and is typically 25 to 100 K greater than the melting temperature or glass transition temperature of the pure polymer. The polymer must be stable at T_i and the diluent should have low volatility at T_i.
2. The solution is formed into the desired shape (flat sheet, tube, or hollow fiber).
3. The solution is cooled at a controlled rate *or* quenched to induce phase separation.
4. The diluent is removed (typically by solvent extraction).
5. The extractant is removed (typically by evaporation) to produce a microporous structure.

This paper focuses on thermally-induced phase separation in a typical system that undergoes liquid–liquid phase separation with subsequent polymer solidification.

0376-7388/91/$03.50 © 1991 Elsevier Science Publishers B.V. All rights reserved.

Thermodynamic considerations

Equilibrium thermodynamic considerations and equilibrium phase diagrams are used here to facilitate the explanation of the dynamic membrane formation process.

Phase equilibria in liquid polymer systems

Liquid–liquid phase separation can occur in systems involving either crystalline or glassy polymers. The major factor determining whether solid–liquid or liquid–liquid phase separation occurs for a system involving a semi-crystalline polymer is the miscibility of the system, which is quantified as the interaction parameter of the semi-crystalline polymer–diluent system [2]. If there is strong polymer–diluent interaction (small interaction parameter), the mixture undergoes solid–liquid phase separation via polymer crystallization when cooled. If there is weak polymer–diluent interaction (great interaction parameter), the blend becomes unstable and undergoes liquid–liquid phase separation to show an upper-critical solution temperature behavior when cooled. In many semi-crystalline polymer–diluent systems, the mixture undergoes liquid–liquid phase separation with subsequent crystallization of the polymer at low initial polymer concentrations and solid–liquid phase separation at high initial polymer concentrations [2,3]. The system discussed in this paper undergoes liquid–liquid phase separation in part of the polymer concentration range.

The criteria for miscibility in any two-component polymer–diluent system can be expressed in terms of the Gibbs free energy of mixing, ΔG_{mix}, and its second derivatives with respect to polymer volume fraction, ϕ_p, at a fixed temperature T and pressure P.

$$\Delta G_{mix} < 0 , \tag{1}$$

$$(\partial^2 \Delta G_{mix}/\partial \phi_p^2)_{T,P} > 0 , \tag{2}$$

where $\Delta G_{mix} = \Delta H_{mix} - T\Delta S_{mix}$, with ΔH_{mix} and ΔS_{mix} representing the enthalpy and entropy of mixing, respectively [4].

If either criterion is not met, the solution may separate into two phases in equilibrium. The criteria expressed above are illustrated in Fig. 1. Three possibilities are shown in Fig. 1: (a) immiscibility throughout the composition range $0 \leqslant \phi_p \leqslant 1$; (b) partial miscibility (that is, immiscibility within the composition range indicated by a negative second derivative); and (c) miscibility across the entire composition range. The three possibilities shown in Fig. 1 can represent three different polymer–diluent systems or one polymer–diluent system at three different temperatures, as discussed in the next paragraph.

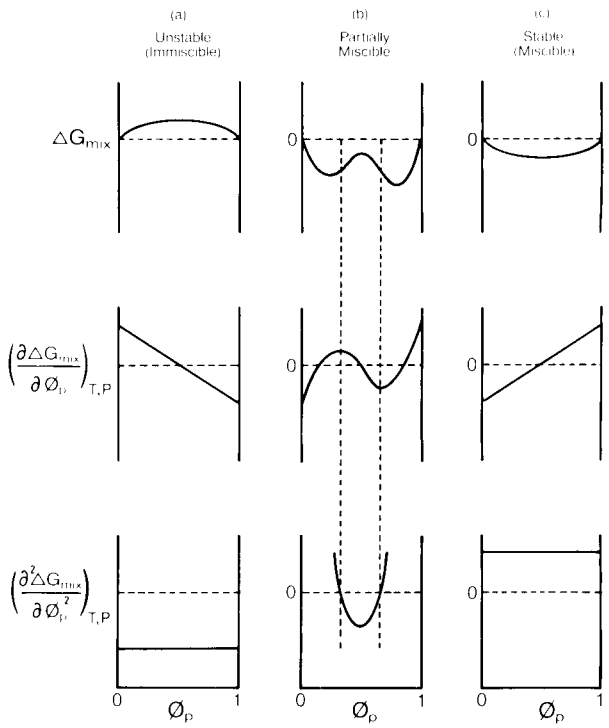

Fig. 1. Gibbs free energy of mixing, first derivative, and second derivative as a function of volume fraction polymer, ϕ_p, at a fixed temperature and pressure; (a) immiscible, (b) partially miscible, (c) miscible.

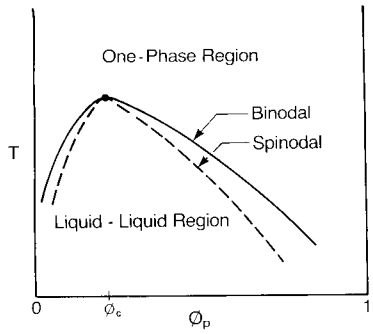

Fig. 3. Temperature-composition phase diagram for a polymer-diluent system showing an upper critical solution temperature (UCST) of composition ϕ_c and liquid-liquid separation in the two-phase region.

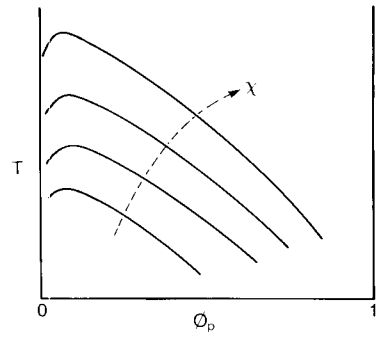

Fig. 4. Effect of strength of interaction on shape and location of binodal; all variables in Eqn. (3) fixed except χ.

ical polymer concentration ϕ_c. The interaction parameter at the critical point is the critical interaction parameter (χ_c), and is used as a criterion of system miscibility. Both ϕ_c and χ_c depend on the size of the polymer and diluent molecules. The binodal (the solid curve in Fig. 3) distinguishes the homogeneous one-phase liquid region from the heterogeneous two-phase liquid–liquid region [5]. In the two-phase region, the system exists as a polymer-rich liquid phase and a polymer-lean liquid phase. The spinodal (the dashed curve in Fig. 3) divides the two-phase region into an *unstable region*, below the spinodal, and a *meta-stable region*, enclosed by the spinodal and the binodal. The terms unstable and meta-stable refer to the solution's ability to resist phase separation and are elaborated upon in the Results and Discussion section below. The Flory-Huggins equation for the polymer–diluent system is

$$\frac{\Delta G_{mix}}{RT}=\frac{\phi_d}{x_d}\ln\phi_d+\frac{\phi_p}{x_p}\ln\phi_p+\chi\phi_d\phi_p\,, \qquad (3)$$

where ΔG_{mix} is the Gibbs free energy of mixing per lattice site, ϕ_d is the volume fraction of the diluent, ϕ_p is the volume fraction of polymer, x_d is the number of lattice sites occupied by a diluent molecule, x_p is the number of lattice sites occupied by a polymer molecule, and χ is the Flory–Huggins interaction parameter [2,4]. The first two terms on the right side of eqn. (3) represent the combinatorial entropy contribution and are always negative. The last term in eqn. (3) represents the enthalpy contribution in the original Flory–Huggins theory and is positive or negative, depending on the sign of χ. If χ is large and positive, ΔG_{mix} becomes positive and demixing occurs. The effect of χ on the shape and location of the binodal is illustrated schematically in Fig. 4. As the polymer–diluent system becomes less compatible (that is, χ becomes more positive) the two-phase region increases in size. Consequently, for a given polymer, the binodal can be shifted to higher temperatures at a fixed polymer concentration or to a greater polymer concentration at a fixed temperature by selecting a less compatible diluent.

General phase diagram

For systems involving a semi-crystalline polymer and a diluent with weak interactions (that is, positive χ), the phase diagram may be represented by Fig. 5. In this diagram, the two-phase liquid–liquid region is located to the left of the monotectic point, ϕ_m, and below the binodal curve. The two-phase solid–liquid region is located to the right of ϕ_m and below the *melting point depression curve*. In this solid–liquid region, as well as below the horizontal broken

In the case of a partially miscible system, a homogeneous one-phase solution is formed only under certain conditions of composition and temperature, as illustrated in Fig. 2. Consider line (c) in Fig. 2. ΔG_{mix} is negative across the entire composition range, indicating miscibility. However, there is an upward bend in the ΔG_{mix}-composition curve between compositions ϕ_b' and ϕ_b'' (that is, between co-tangential points in the curve). In the region where ΔG_{mix} of the homogeneous solution is greater (that is, less negative) than that of a combination of two phases with compositions ϕ_b' and ϕ_b'', minimum free energy can be attained via phase separation. Thus, mixtures of initial composition between ϕ_b' and ϕ_b'' separate into two phases of composition ϕ_b' and ϕ_b''. Since the two resulting phases are in equilibrium, they have the same chemical potential (defined as the derivative of the Gibbs free energy of mixing with respect to composition), as indicated by a common tangent.

The second derivative of ΔG_{mix} is negative between compositions ϕ_s' and ϕ_s'' (that is, between inflection points in the ΔG_{mix}-composition curve), indicating the system is *unstable* in this composition range. There is a spontaneous phase separation in this region. The second derivative of ΔG_{mix} is positive between compositions ϕ_b' and ϕ_s', and between compositions ϕ_s'' and ϕ_b''. There is no spontaneous phase separation in this region, since the system is stable to small concentration fluctuations. Phase separation can take place where there is a concentration fluctuation large enough to overcome the energy barrier. The system in this region is *meta-stable.*

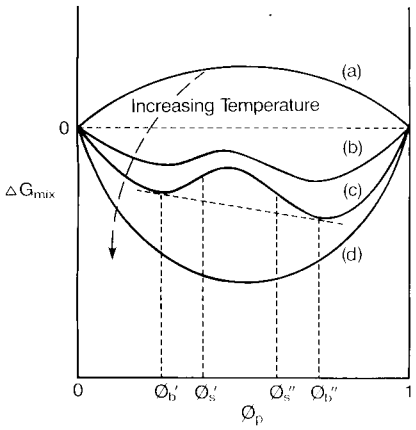

Fig. 2. Gibbs free energy of mixing as a function of volume fraction of polymer. Note minima, ϕ_b' and ϕ_b'', common tangent (equilibrium phases of equal chemical potential), inflection points ϕ_s' and ϕ_s'', and the influence of temperature for a system possessing an upper critical solution temperature; (a) immiscible, (b) and (c) partially miscible, (d) miscible.

The effect of temperature on a partially miscible system exhibiting an upper critical solution temperature is shown in Fig. 2. At elevated temperatures, there is sufficient thermal energy to achieve solvation throughout the entire composition range. As the temperature is decreased and thermal energy is removed, the strength of the polymer–diluent interactions is decreased. Consequently, the polymer molecules and the diluent molecules retract from each other, and phase separation occurs within the composition range bracketed by the co-tangential points.

If the locus of co-tangential points in Fig. 2 is plotted in the form of a temperature–composition phase diagram, the curve is referred to as the *binodal.* If the locus of inflection points is similarly plotted, the curve is referred to as the *spinodal.* In Fig. 3, the binodal and spinodal are shown for a system displaying an upper critical solution temperature. The maximum temperature at which a two-phase liquid–liquid mixture can exist is the upper critical solution temperature, which occurs at a polymer concentration of ϕ_c. The critical point is defined as the point at which the binodal and the spinodal curves meet. This point satisfies the criteria of $(\partial^2 \Delta G_{mix}/\partial \phi_p^2)_{T,P}=0$, $(\partial^3 \Delta G_{mix}/\partial \phi_p^3)_{T,P}>0$, and $(\partial^4 \Delta G_{mix}/\partial \phi_p^4)_{T,P}=0$ [5]. This point is unique for each polymer–diluent system and is denoted by the critical temperature T_c and crit-

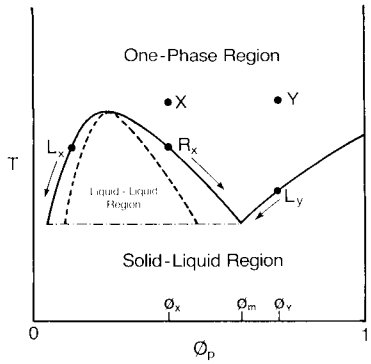

Fig. 5. Temperature–composition phase diagram for a system showing liquid–liquid and solid–liquid phase separation. Note monotectic point, ϕ_m.

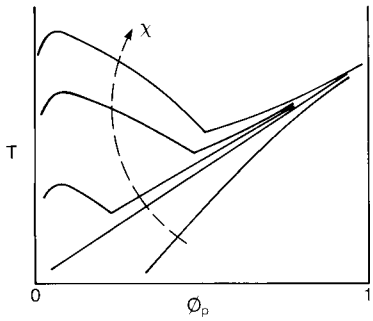

Fig. 6. Effect of χ on shape of the general phase diagram and the location of the monotectic point.

line, the diluent is not capable of dissolving all of the polymer, and the polymer crystallizes.

Combining Figs. 4 and 5 in Fig. 6 shows the effect of χ on the shape of the general phase diagram for the hypothetical case where all other variables are constant. Note that ϕ_m increases as χ increases. In terms of control of membrane formation, Fig. 6 indicates for a given polymer at a specific concentration, the mechanism of phase separation can be changed from solid–liquid to liquid–liquid with subsequent polymer crystallization through the appropriate choice of diluent. As discussed below, the mechanism of phase separation significantly alters the resulting membrane structure.

Non-equilibrium phase diagrams

Since TIPS membrane formation is a non-equilibrium process, the cooling rate effects on the phase diagram must be considered. At experimentally controllable cooling rates, the cooling rate has a relatively minor effect on the liquid–liquid phase separation temperature and the location of the cloud point curve (which is assumed to be representative of the binodal curve) [6], as illustrated in Fig. 7 for the isotactic polypropylene (iPP)–n,n-bis(2-hydroxyethyl) tallowamine (TA) system. However, the cooling rate does have a significant effect on the temperature at which the solid–liquid phase separation occurs as shown in Fig. 7. Cooling at any finite rate permits supercooling; that is, the solution is cooled to a temperature below its corresponding equilibrium crystallization temperature prior to the actual crystallization of the polymer from solution. In this case, the apparent crystallization temperature is less than the equilibrium melting temperature. In terms of an experimentally determined non-equilibrium phase diagram, supercooling is represented by a depressed apparent T_c of the pure polymer, a depressed crystallization curve

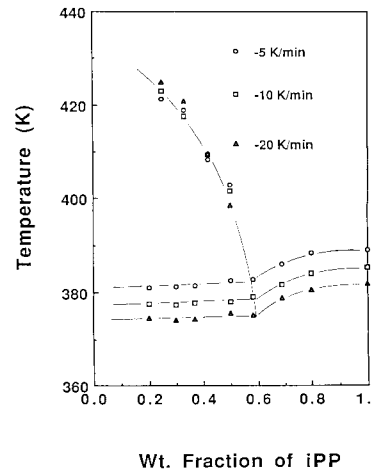

Fig. 7. Effect of cooling rate on freezing point depression curve and demarkation between the liquid–liquid and solid–liquid regions for iPP–TA system.

(defined as the crystallization temperature–concentration curve), and a depressed horizontal solid–liquid line beneath the liquid–liquid region. Note in Fig. 7 ϕ_m shifts slightly to greater polymer concentrations as the cooling rate increases.

In terms of control of membrane formation, Fig. 7 indicates for a given polymer–diluent system of concentration in the range near ϕ_m, the mechanism of phase separation (solid–liquid versus liquid–liquid) may be altered through the appropriate choice of cooling rate. For example, a polymer–diluent blend of polymer concentration slightly greater than ϕ_m would undergo solid–liquid phase separation when slowly cooled but may undergo liquid–liquid phase separation when rapidly cooled or quenched. As discussed below, the mechanism of phase separation significantly alters the resulting membrane structure.

Materials and methods

Microporous isotactic polypropylene (iPP, weight average molecular weight 243,000, melting point 449 K, Himont "Pro-fax 6723") membranes were prepared by liquid–liquid phase separation from melt blends with n,n-bis (2-hydroxyethyl) tallowamine (TA, initial boiling point > 573 K, Armak Chemicals Armostat 310) and extracted with 1,1,1-trichloroethane (TCE, reagent grade Ashland Chemical Co.). The materials were used as received with no further purification.

Methods

The procedures for determining the crystallization curves, for forming membrane samples in a compression mould, and for preparing the membrane samples for scanning electron microscopic characterization have been described in the first paper in this series [1]. The cloud point curves, representing the binodals, were experimentally determined using *thermo-optical microscopy*, the schematic diagram of which is shown in Fig. 8. In this method, a thin sample of the polymer–diluent mixture was placed between two microscope slide cover slips, placed in a Mettler FP-82 hot stage, and heated to 493 K. After 20 to 30 sec, the cover slips were gently pressed to cause the sample to spread and form a sample as thin as possible. The cover-slip assembly was cooled, removed from the hot stage, and visually inspected to assure uniformity. The cover-slip assembly containing the uniformly spread sample was again placed in the hot stage, heated to 473 K, and maintained at this temperature for at least 5 min to assure homogeneity of the melt. Light was passed through the sample and the intensity of the transmitted light was monitored as the temperature of the sample was decreased at 10 K/min to a final temperature of 373 K. The experiment was conducted with unpolarized light of wave length 628 nm. The intensity of the transmitted light decreased as the liquid–liquid phase separation occurred. The onset of the signal change was used as an indication of the onset of the liquid–liquid phase separation.

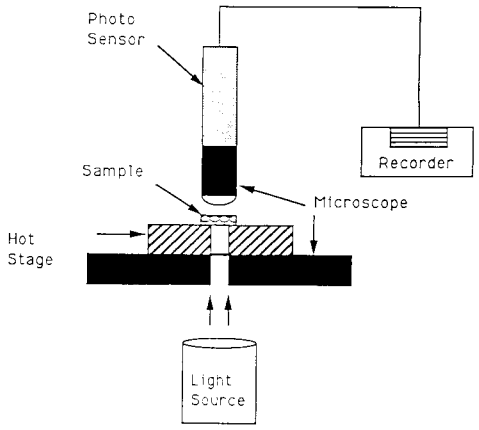

Fig. 8. A schematic diagram of thermo-optical microscope.

Results and discussion

The 10 K/min phase diagram for the iPP–

TA system, shown in Fig. 7, displays a monotectic point at approximately 59 wt.% iPP. For polymer concentrations less than 59 wt.%, a cloud point curve is shown above the horizontal crystallization curve (that is, the crystallization temperature is independent of composition at polymer concentrations less than 59 wt.%). Cloud points at concentrations less than the critical point have not been determined due to experimental difficulties and because useful membranes cannot be prepared from solutions in this concentration range. Upon cooling a homogeneous melt of polymer concentration less than 59 wt.%, liquid–liquid phase separation occurs followed by crystallization of the polymer-rich phase when the temperature falls below 378 K, as indicated in Fig. 7. Upon cooling a homogeneous solution of polymer concentration greater than 59 wt.%, solid–liquid phase separation occurs at the crystallization curve. In the following paragraphs, membranes prepared by slowly cooling and by rapidly quenching 25 and 70 wt.% iPP mixtures are discussed.

Membranes were prepared from a 25 wt.% iPP mixture cooled at 10 K/min from 533 K to 318 K. The resulting structure of spherical cells connected by circular pores is shown in Fig. 9. The cells represent the cavities left behind by the extracted diluent, the pores connecting the cells are speculated to be the result of the collision of growing polymer-lean droplets, and the cell walls are semi-crystalline iPP. The *cellular structure* shown in Fig. 9 has also been reported by Hiatt et al. [7]. They melt blended iPP with TA in the concentration range 21 to 30 wt.% iPP and induced phase separation by casting the hot solution onto a warm surface. Although no direct experimental evidence of the sequence of events leading to the cellular structure shown in Fig. 9 exists currently, it is possible to speculate on the membrane formation mechanism as follows. The 10 K/min cooling process is represented schematically in Fig. 5 by the semi-crystalline polymer–diluent mixture of composition ϕ_x heated to an elevated temperature represented by the point X. Upon *slow cooling*, the solution crosses the binodal curve and enters the region between the binodal and spinodal curves. In this region, which corresponds to a point between ϕ_s'' and ϕ_b'' in Fig. 2, the solution is relatively stable (meta-stable) to small fluctuations in local concentration. However, the solution is unstable to concentration fluctuations that result in at least one region of local concentration near the opposite side of the binodal curve; that is, local regions of concentration between ϕ_b' and ϕ_s' in Fig. 2 [6,8]. This region of anomalous concentration, which is capable of decreasing the total free energy of the system, is referred to as a nucleus and is close to pure diluent. As cooling continues to lower temperatures, the polymer-lean nuclei grow in size through diffusion of diluent, and the droplet composition follows the left branch of the binodal curve (as represented in Fig. 5 by L_x). Simultaneously, the composition of the surrounding polymer-rich phase follows the right branch of the binodal curve (as represented in Fig. 5 by R_x). In this way, the solution becomes a dispersion of droplets of the polymer-lean phase in a continuous polymer-rich phase. When the temperature drops below the horizontal solid–liquid line under the liquid–liquid phase separation region, iPP crystallizes out of the polymer-rich phase to form the spherulites, and the grown polymer-lean droplets are entrapped within the iPP spherulites [9,10]. Without direct experimental evidence, it is impossible to attribute with any confidence the structure shown in Fig. 9 as resulting from this *nucleation and growth mechanism*. It remains to be established experimentally whether 10 K/min represents *slow cooling*.

The membrane shown in Fig. 9 was further investigated under crossed polar illumination [11]. A Maltese-cross pattern indicative of birefringent spherulitic structure was observed, and the presence of the spherulites was con-

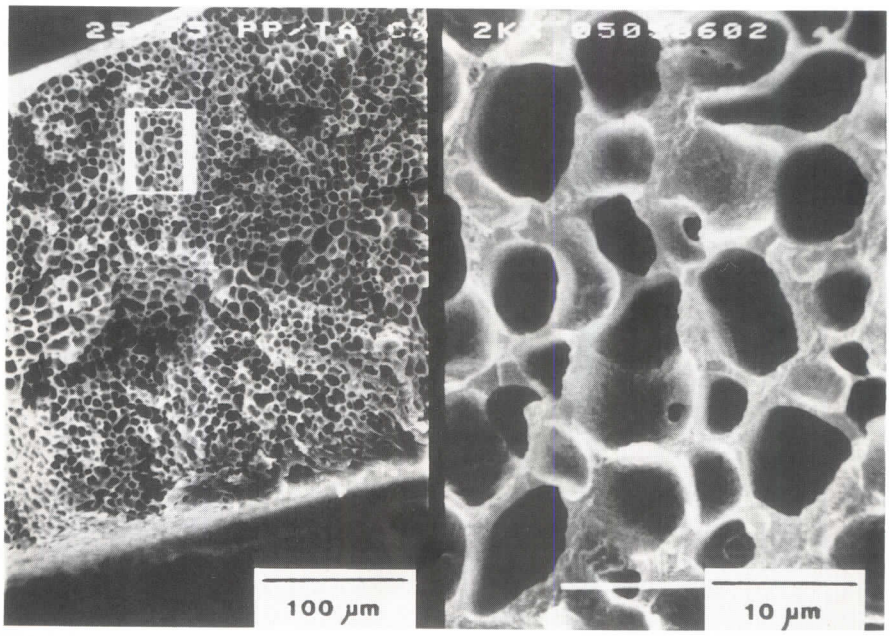

Fig. 9. Split-image scanning electron photomicrograph of the cellular structure resulting from liquid–liquid phase separation of a 25 wt.% iPP in iPP–TA solution cooled from 533 K to 318 K at 10 K/min in a Mettler FP-82 hot stage. (Diluent was extracted with TCE).

firmed. The size of the spherulite was the same as the large scale structure evident in the low magnification portion of Fig. 9 and much larger than the entrapped droplets.

When a mixture of the same composition as discussed in the previous paragraph (25 wt.% iPP) was melt blended at the same temperature (533 K) and quenched at 318 K in water, the *lacy structure* shown in Fig. 10 resulted. Again, although no direct experimental evidence of the sequence of events leading to the lacy structure shown in Fig. 10 exists currently, it is possible to speculate on the membrane formation mechanism as follows. The quench process is represented schematically in Fig. 5 by the semi-crystalline polymer–diluent mixture of composition ϕ_x heated to an elevated temperature represented by the point X. Upon *rapid cooling*, the solution crosses the binodal and the spinodal curves and enters the unstable region. In this region, which corresponds to composition between ϕ'_s and ϕ''_s in Fig. 2, $(\partial^2 \Delta G_{mix}/\partial \phi_p^2)_{T,P}$ is negative, and the solution is unstable to even the smallest concentration fluctuations. The theory of spinodal decomposition, as developed by Cahn [12,13] predicts small fluctuations in concentration of wavelength greater than a certain crucial value spontaneously increases in amplitude. Consequently, the size of the new phase stays roughly the same, while its concentration deviation from the bulk increases. Cahn also showed the rate of increase in amplitude depends on the fluctuation wavelength. Thus, the solution separates spontaneously into tiny, co-continuous polymer-lean phases of composition ϕ'_b and polymer-rich phases of composition ϕ''_b (viscous constraints may prevent the actual attainment of these compositions). Without direct experimental evidence, it is impossible to attribute with any

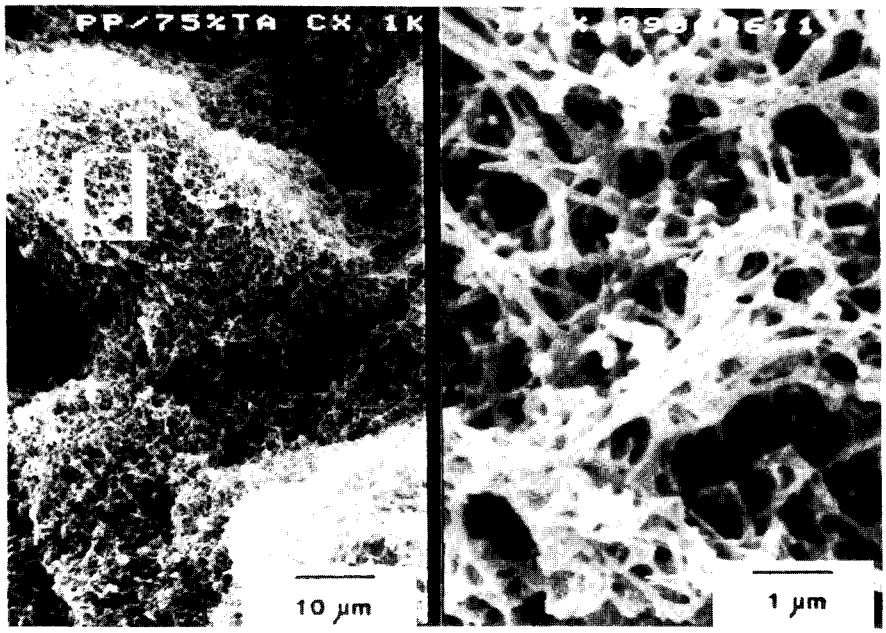

Fig. 10. Split-image scanning electron photomicrograph of the lacy structure resulting from liquid–liquid phase separation of a 25 wt.% iPP in iPP–TA solution quenched from 533 K to 318 K in water. Left: low magnification; right: high magnification. (Diluent was extracted with TCE).

confidence the lacy structure shown in Fig. 10 as resulting from the *spinodal decomposition mechanism*. It remains to be established experimentally whether the quenching technique applied in this study represents *rapid cooling*.

Since the quench temperature (318 K) is below the iPP crystallization temperature, as shown in Fig. 7, the liquid–liquid TIPS is accompanied by iPP crystallization. Optical microscopy reveals the iPP comprising the lacy matrix in Fig. 10 is spherulitic. Indications of this spherulitic macrostructure are seen in the lower magnification image of Fig. 10. The occurrence of crystallization on the same time scale as the liquid-liquid phase separation may explain the inability of the phase separated domains to grow in size via coarsening or any other mechanism.

Membranes were prepared from a 70 wt.% iPP mixture and either quenched from 473 K to 331 K (Fig. 11) or cooled at 10 K/min from 473 K to 331 K (Fig. 12). Both processes are represented schematically in Fig. 5 by the semi-

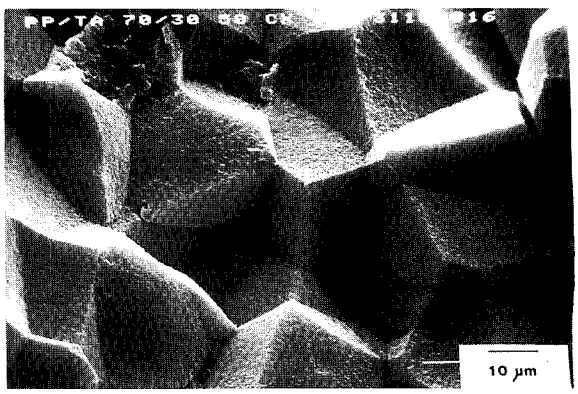

Fig. 11. Scanning electron photomicrograph of the spherulitic structure resulting from the rapid solid–liquid phase separation of a 70 wt.% iPP in iPP–TA solution quenched from 473 K to 331 K in water. (Diluent was extracted with TCE).

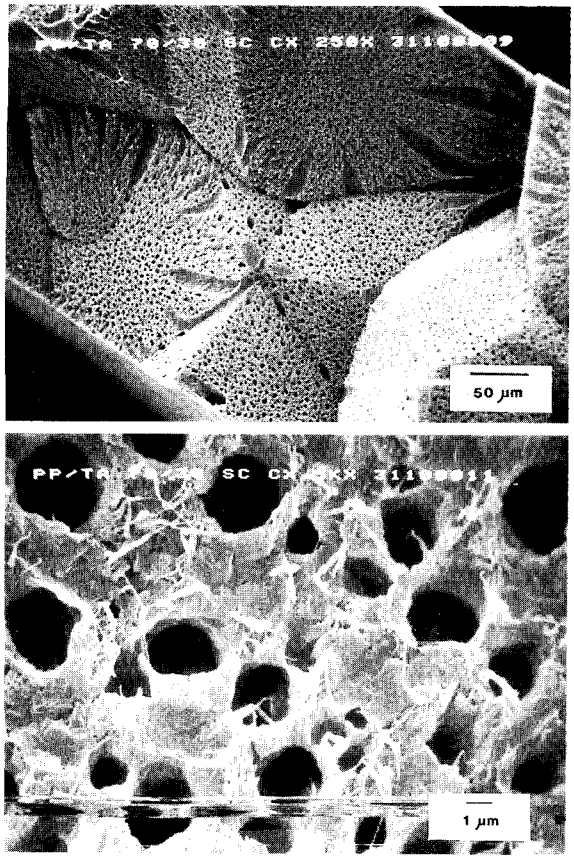

Fig. 12. Split-image scanning electron photomicrograph of the spherulitic structure resulting from the slow solid–liquid phase separation followed by liquid–liquid phase separation of a 70 wt.% iPP in iPP–TA solution cooled from 473 K to 331 K at 10 K/min in a Mettler FP-82 hot stage. Top: low magnification; bottom: high magnification. (Diluent was extracted with TCE).

crystalline polymer–diluent mixture of composition ϕ_y heated to an elevated temperature represented by point Y. At the conditions represented by Y, the mixture is a true homogeneous solution. Upon removal of thermal energy, the solution undergoes *solid–liquid* phase separation into essentially pure polymer crystals in a liquid phase represented by L_y. As the temperature is decreased, the liquid phase (comprised of diluent and amorphous polymer) follows the melting point depression curve until the monotectic point is reached. Below the monotectic temperature, the remaining solution phase undergoes liquid–liquid phase separation as described above. Quenching yielded truncated spherulites with textured surfaces, as shown in Fig. 11. Cooling at 10 K/min yielded truncated spherulites with more open surfaces than produced via quenching. Investigation of the surfaces of the spherulites produced via slow cooling revealed a cellular structure (Fig. 12, bottom). The difference in spherulitic surface structure is tentatively attributed to differences in the phase separation mechanism experienced by the solution phase represented by L_y; however, further experimentation is required to resolve this issue. The spherulites produced via slow cooling are considerably larger than those resulting from the quench process because of the fewer nuclei produced and the longer growth period in the case of the slow cooling (see discussion in Ref. [1]).

Conclusions

The dynamic phase diagrams at 10 K/min cooling were determined for iPP–TA. The monotectic point of iPP–TA system is 59 wt.% iPP and 378 K. At iPP compositions less than the monotectic composition iPP–TA samples yielded a lacy structure when quenched and a cellular structure when slowly cooled. At compositions greater than monotectic composition, iPP–TA samples yielded a spherulitic structure without discernible pores when quenched and a larger spherulitic structure with a cellular surface when slowly cooled.

Acknowledgements

The authors gratefully acknowledge the valuable comments and suggestions made by Dave Gagnon, Gene Shipman, and Mike Tseng of 3M as well as Joel Barlow of The University of

Texas at Austin. We also wish to express our gratitude to Steve Pittman of 3M for the photomicrographs. Finally, the continued funding of this project by 3M and the Texas Advance Technology Program is sincerely appreciated.

References

1 D.R. Lloyd, K.E. Kinzer and H.S. Tseng, Microporous membrane formation via thermally induced-phase separation. I. Solid-liquid phase separation, J. Membrane Sci., 52 (1990) 239.

2 S.S. Kim and D.R. Lloyd, Thermodynamics of polymer-diluent systems for thermally-induced phase separation. III. Liquid-liquid phase separation systems, Polymer, in press.

3 W.R. Burghardt, Phase diagrams for binary systems exhibiting both crystallization and limited liquid-liquid miscibility, Macromolecules, 22 (1989) 2482.

4 P.J. Flory, Principles of Polymer Chemistry, Cornell University Press, Ithaca, NY, 1953, Chap. 13.

5 I.C. Sanchez, Polymer phase separation, in: Encyclopedia of Physical Science and Technology, Vol. 11, Academic Press, New York, NY, 1981, 1-18.

6 R. Koningsveld and A.J. Staverman, Liquid-liquid phase separation in multi-component polymer solutions. IV. Coexistence curve, Kolloid-Z. u. Z. Polymere, 218 (1967) 114.

7 W.C. Hiatt, G.H. Vitzthum, K.B. Wagener, K. Gerlach and C. Josefiak, Microporous membranes via upper critical temperature phase separation, in: D.R. Lloyd (Ed.), Materials Science of Synthetic Membranes, ACS Symp. Ser. No. 269, American Chemical Society, Washington, DC, 1985, pp. 229-244.

8 R. Koningsveld and A.J. Staverman, Determination of critical points in multi-component polymer solutions, J. Polym. Sci., Part C, Polym. Symp., 16 (1967) 1775.

9 N. Inaba, K. Sato, S. Suzuki and T. Hashimoto, Morphological control of binary polymer mixtures by spinodal decomposition and crystallization. 1. Principle of method and preliminary results on PP/EPR, Macromolecules, 19 (1986) 1690.

10 N. Inaba, T. Yamada, S. Suzuki and T. Hashimoto, Morphological control of binary polymer mixtures by spinodal decomposition and crystallization. 2. Further studies on polypropylene and ethylene-propylene random copolymer, Macromolecules, 21 (1988) 407.

11 K.E. Kinzer and D.R. Lloyd, Thermally-induced phase separation mechanisms for microporous membrane formation, Proc. of the ACS Division of Polymeric Materials: Science and Engineering, Vol. 61, American Chemical Society, Washington DC, 1989, pp. 794-798.

12 J.W. Cahn, On spinodal decomposition, Acta Met., 9 (1961) 795.

13 J.W. Cahn, Phase separation by spinodal decomposition in isotropic systems, J. Chem. Phys., 42 (1965) 91.